

See discussions, stats, and author profiles for this publication at: <https://www.researchgate.net/publication/228949707>

# Time-Dependent Density Functional Theory Study on Polyazopyrrole and Polyazothiophene

ARTICLE in MACROMOLECULES · NOVEMBER 2003

Impact Factor: 5.8 · DOI: 10.1021/ma034564+

---

CITATIONS

26

---

READS

15

3 AUTHORS, INCLUDING:



Zhengxi Zhu

Yangzhou University

16 PUBLICATIONS 311 CITATIONS

SEE PROFILE



Yun Lu

KAI Research, Inc. An Altarum Company

99 PUBLICATIONS 1,558 CITATIONS

SEE PROFILE

# Time-Dependent Density Functional Theory Study on Polyazopyrrole and Polyazothiophene

Zhengxi Zhu, Yongfeng Wang, and Yun Lu\*

State Key Laboratory of Coordination Chemistry, Department of Polymer Science and Engineering, Nanjing University, Nanjing 210093, P. R. China

Received May 2, 2003; Revised Manuscript Received September 8, 2003

**ABSTRACT:** Two narrow band gap polymers, polyazopyrrole (PAPY) and polyazothiophene (PATH), were theoretically investigated by means of time-dependent density functional theory (TDDFT) with the B3LYP functional. The most stable trans conformation that would be dominant in the infinite length polymer was discerned, and the chain length dependence of excitation energies of oligomers was studied. By extrapolation, the band gaps of the corresponding trans forms of PAPY and PATH were found to be as low as 1.12 and 0.98 eV, respectively. IR spectra of the oligomers were successfully simulated by density functional theory (DFT) with the B3LYP functional. The results are in good agreement with the reported experimental ones.

## 1. Introduction

Since the discovery of metallic conductivity in doped polyacetylene,<sup>1,2</sup> increasing attention has been focused on  $\pi$ -conjugated polymers because of their many interesting properties such as high intrinsic conductivities, excellent nonlinear optical properties and electroluminescence, and so forth.<sup>3</sup> In particular, intensive research has been dedicated to exploring novel conjugated polymers with narrow band gaps.<sup>4–6</sup> Polyacetylene, which consists of alternate single and double carbon–carbon bonds, is the simplest model of this kind of materials, and its band gap should be ideally zero by using a simple Hückel approximation.<sup>7</sup> According to Peierls theory, however, such a one-dimensional structure is unstable and the coupling of electrons and phonons with lattice distortions leads to a localization of single and double bonds which lifts the degeneracy and results in a localization of  $\pi$ -electronics with the opening of a band gap ( $E_g$ ).<sup>8</sup> In the past two decades, a large number of studies have been performed both experimentally and theoretically by introducing fused ring systems, ladder-type structures or electron acceptor units, and so forth into  $\pi$ -conjugated backbone chains, aiming at decreasing the band gap value to near zero to present a true “organic conductor” without dopants.<sup>5,9</sup>

The polyazoheteroaromatic system is a member of the group of narrow band gap conducting polymers. It is derived from a diheteroaromatic by inserting an azo group among the dimer heteroaromatic rings (as shown in Figure 1). Since the first successful synthesis in 1995 by Yokomichi et al.,<sup>10</sup> polyazopyrrole has possessed the narrowest band gap among the neutral pyrrole-based conducting polymers in experiments until now. In 1996, the polyazopyrrole films were investigated by Zotti et al. by using techniques of cyclic voltammetry (CV) and infrared (IR) and UV–vis–NIR spectroscopies with the objective of studying materials with high intrinsic conductivity.<sup>11</sup> The obtained polyazopyrrole (PAPY) presents a significant decrease in energy gap from 2.85 eV<sup>12</sup> of polypyrrole to about 1.0 eV.<sup>11</sup> After that, Nero

gave the theoretical simulation of the electronic absorption spectra of polyazopyrrole.<sup>13</sup> We tentatively extrapolated the first optically active transition energies of azopyrrole oligomers in Nero's theoretical study (Figure 4 in ref 13) and found that the resulting  $E_g$  is 0.8 eV larger than the experimental  $E_g$  (about 1.0 eV<sup>11</sup>). Furthermore, it is very interesting to understand why polyazopyrrole shows the narrow band gap and if other azoheteroaromatic polymers also bear a resemblance to it.

In addition, the azo groups on the backbone of the conducting chain can be the basis for the molecular switches, so the polyazoheteroaromatic system can be a promising candidate for the fabrication of molecular devices. There should be two relatively stable ground-state trans conformations of polyazopyrrole, as shown in Figure 2a and b, even though this has never been mentioned in previous studies. Discerning the most stable trans conformation is necessary for future investigations on the trans/cis reversible interconversion<sup>14,15</sup> of azo groups under external light or heat stimulus in this system.

In consideration of all these merits, inspiring perspective, and the problems mentioned above, we made a trial to theoretically investigate polyazopyrrole. At the same time, we also attempted to study a new polymer, polyazothiophene (as shown in Figure 2c and d), in the same way as we did in the case of study of polyazopyrrole.

In this paper, we discerned the most stable trans conformation that would be dominant in the corresponding infinite length polyazopyrrole and polyazothiophene for the first time. TDDFT with the B3LYP functional was employed to study the chain length dependence of the vertical excitation energies of azopyrrole and azothiophene oligomers, and the theoretical prediction on the band gaps of the corresponding infinite trans polymers was obtained by extrapolation. IR spectra of oligomers were successfully simulated using DFT with the B3LYP functional. The effective conjugation lengths (ECLs) were estimated by the convergence of excitation energy with the chain length within a threshold of 0.01 eV.

\* Corresponding author. Phone: 86-25-83592569. Fax: 86-25-83317761. E-mail: yunlu@nju.edu.cn.

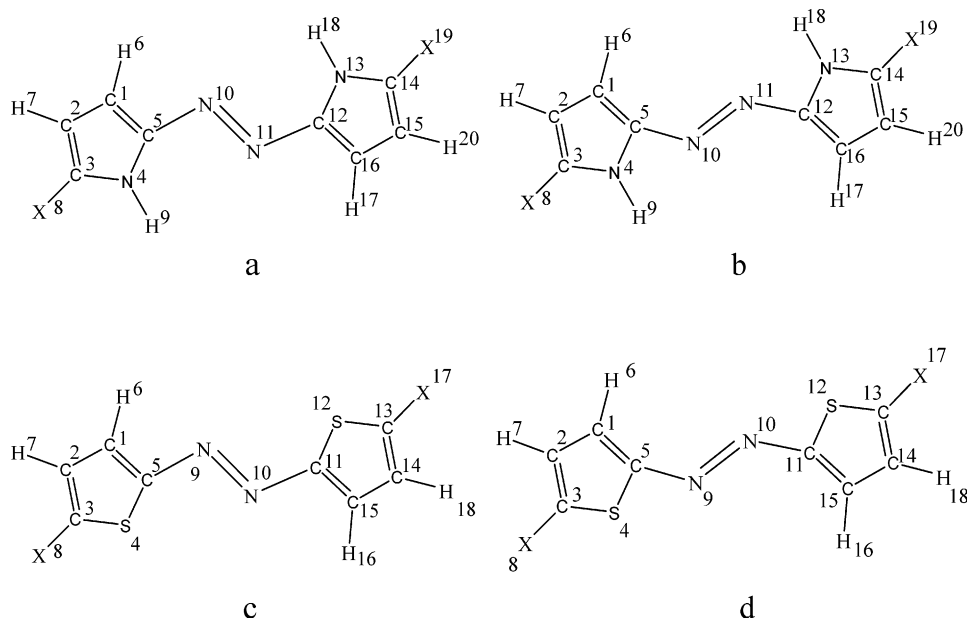


**Figure 1.** Two stable, anticoplanar ground-state trans conformations of azopyrrole and azothiophene monomers: (a) APYb; (b) APYb; (c) ATHa; (d) ATHb (X = H).

## 2. Models and Computational Methods

The  $E_g$  values of the conducting polymers are usually determined from the low-energy absorption edge of the electronic absorption spectra in experiments.<sup>11</sup> The theoretical quantity of  $E_g$  for direct comparison with the experimental band gap should be the transition (or excitation) energy from the ground state to the first dipole-allowed excited state. There exist various theoretical approaches for simulating band gaps of oligomers as well as of infinite polymers. The crudest estimate, but most widely used due to its cheapness, is on the basis of the orbital energy difference between the highest occupied molecular orbital (HOMO) and the lowest unoccupied molecular orbital (LUMO), obtained from Hartree–Fock (HF) or density functional theory (DFT) calculations.<sup>16,17</sup> The implicit assumption underlying this approximation is that the lowest singlet excited state can be described by only one singly excited configuration in which an electron is promoted from the HOMO to the LUMO. In addition, the orbital energy difference between the HOMO and the LUMO is still an approximate estimate of the transition energy, since the transition energy also contains significant contributions from some two-electron integrals. However, the real situation is that an accurate description of the lowest singlet excited state requires a linear combination of a number of excited configurations. Although the calculated HOMO–LUMO gap agrees fairly well with the experimental band gap in many cases,<sup>17</sup> this may probably be due to the error cancellations. There are also other more elaborate theoretical methods. Among them, Hartree–Fock (HF)-based methods, such as the configuration interaction singles (CIS) method<sup>18</sup> and the random phase approximation (RPA),<sup>19</sup> which is equivalent to the time dependent HF (TDHF) method,<sup>20</sup> usually only provide qualitative or semiquantitative descriptions for the low-lying excited states.<sup>21</sup>

Fortunately, a recently developed tool, time-dependent density functional theory (TDDFT),<sup>22,23</sup> was a success to some degree. The fusion of a significant quantitative improvement and moderate computational cost has attracted the increasing favor of chemists. Over the

past few years, it has advanced to one of the most popular theoretical approaches to calculate excited-state properties of medium-sized and large molecules up to about 200 second-row atoms.<sup>24,25</sup> Especially for excited states below the Rydberg threshold, TDDFT with improved correctly asymptotic functionals can usually bring out impressive results.<sup>24–28</sup> Let us briefly review the calculating excitation energies with the TDDFT scheme. For real Kohn–Sham orbitals, excitation energies  $\omega$  within the TDDFT scheme can be determined by solving the non-Hermitian eigenvalue equation of the form<sup>29,30</sup>

$$\begin{pmatrix} A & B \\ B & A \end{pmatrix} \begin{pmatrix} X \\ Y \end{pmatrix} = \omega \begin{pmatrix} 1 & 0 \\ 0 & -1 \end{pmatrix} \begin{pmatrix} X \\ Y \end{pmatrix}$$

For a general hybrid HF/DFT functional, the elements of the matrices are formally written as<sup>29</sup>

$$A_{ia\sigma,jb\tau} = \delta_{ij}\delta_{ab}\delta_{\sigma\tau}(\epsilon_{a\sigma} - \epsilon_{i\tau}) + (i_{\sigma}a_{\sigma}|j_{\tau}b_{\tau}) - \delta_{\sigma\tau}c_{\text{HF}}(i_{\sigma}j_{\sigma}|a_{\tau}b_{\tau}) + (1 - c_{\text{HF}})(i_{\sigma}a_{\sigma}|f_{\sigma\tau}|j_{\tau}b_{\tau}) \quad (1)$$

$$B_{ia\sigma,jb\tau} = (i_{\sigma}a_{\sigma}|b_{\tau}j_{\tau}) - \delta_{\sigma\tau}c_{\text{HF}}(i_{\sigma}b_{\sigma}|a_{\tau}j_{\tau}) + (1 - c_{\text{HF}})(i_{\sigma}a_{\sigma}|f_{\sigma\tau}|b_{\tau}j_{\tau}) \quad (2)$$

where  $i$  and  $j$  are used for ground-state occupied orbitals,  $a$  and  $b$  are for virtual orbitals, and  $\sigma$  and  $\tau$  are the spin variables.  $\epsilon$  refers to the ground-state orbital energy, and  $c_{\text{HF}}$  is the coefficient of the HF exchange part in the functional. In eq 1, the first term is the energy difference between virtual orbital  $a$  and occupied orbital  $i$ . The second term of eq 1 describes the Coulomb repulsion between singly excited configurations. The third term of eq 1 originates from the nonlocal HF exchange part of the Kohn–Sham operator and has the appearance of a Coulombic term, since the created holes (orbitals  $i$  and  $j$ ) interact with the electrons (orbitals  $a$  and  $b$ ), which directly corresponds to the electrostatic attraction within the excited state of ionic character.<sup>29</sup> The last terms in the two above equations are in the adiabatic approximation defined as

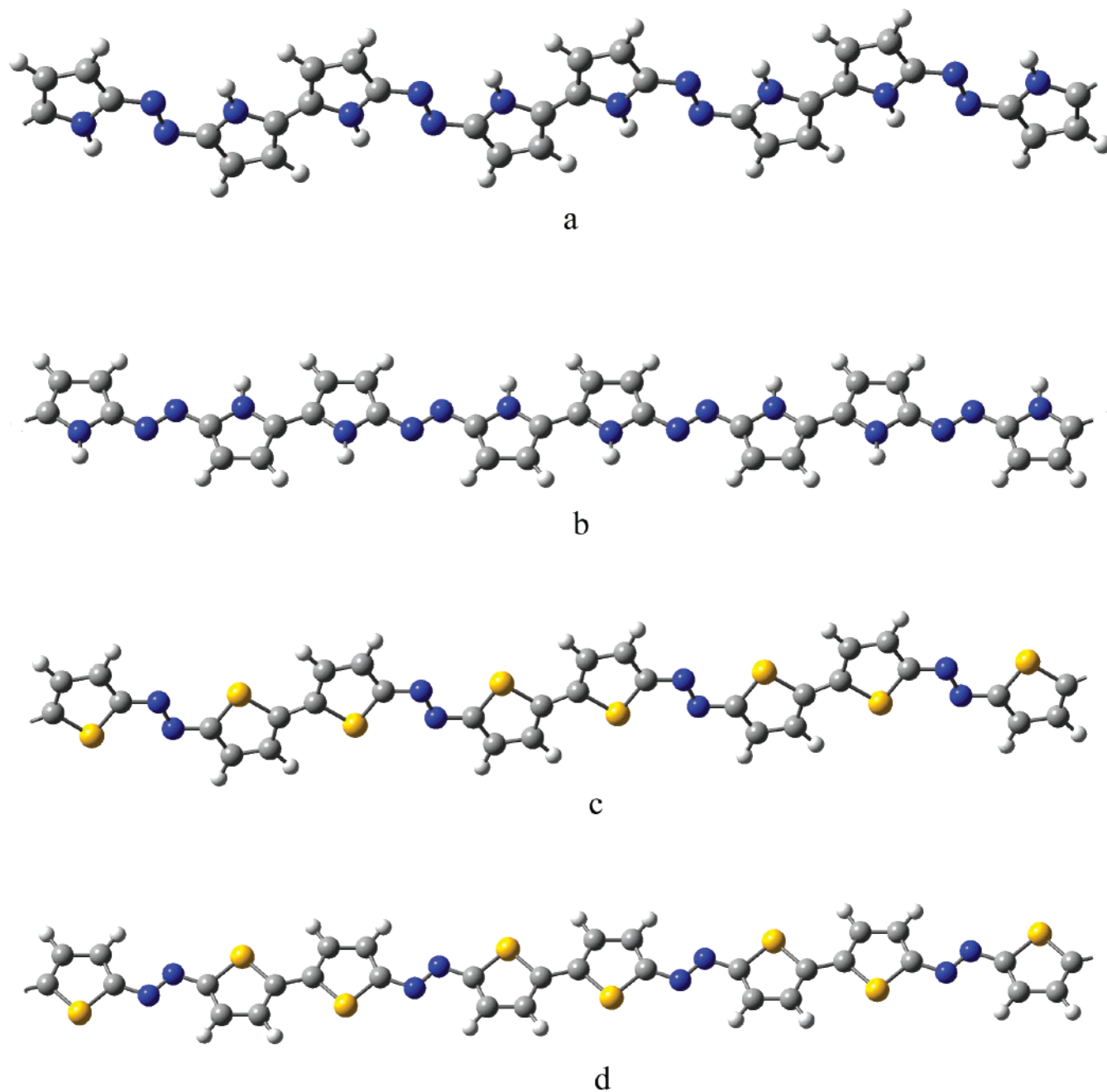


**Figure 2.** Two stable, anticoplanar ground-state trans conformations of polyazopyrrole and polyazothiophene: (a) PAPYa; (b) PAPYb; (c) PATHa; (d) PATHb.

$$(i_{\sigma}a_{\sigma}|f_{\sigma\tau}|j_{\tau}b_{\tau}) =$$

$$\int \int \phi_i(r_1) \phi_a(r_1) f_{\sigma\tau}(r_1, r_2) \phi_j(r_2) \phi_b(r_2) dr_1 dr_2 \quad (3)$$

where  $f_{\sigma\tau}(r_1, r_2)$  is the nonlocal XC kernel. TDDFT is a formally exact theory, but since the exact exchange-correlation (XC) functional is in fact unknown, approximate XC functionals must be employed. Thus, the nonlocal XC kernel is usually further approximated by using local XC functionals, such as the SVMN functional, resulting in the local density approximation (LDA).<sup>22,23</sup> Although the introduction of gradient-corrected density functionals such as BLYP gives an overall improvement to the XC energies of the LDA, the gradient-corrected potentials are still local.<sup>29</sup>

For the lowest-lying singlet excitation energies of our investigated  $\pi$ -conjugated system, the TDDFT scheme with conventional functionals also bears some deficiencies,

because of the employed LDA. First, the LDA induces the XC potential to exponentially decay (the true potential decays Coulombically like  $1/r$ ) and to vanish at long spatial distances.<sup>26,29–34</sup> That case also can directly be seen from the exponential decay of the density itself.<sup>31</sup> As a consequence, spatially extended Rydberg states are only poorly described with TDDFT employing these asymptotically incorrect functionals.<sup>26,29,33,34</sup> Recently, it was also pointed out that TDDFT with an incorrectly asymptotic XC potential can yield substantial errors for valence excited states of spatially extended  $\pi$ -conjugated systems.<sup>32</sup> In addition, excitation energies to the lowest singlet excited states calculated by TDDFT with the pure XC functionals may tend to converge to the same value with the corresponding HOMO–LUMO gaps for infinite polymers or sufficiently large systems.<sup>21,30</sup> All these failures resulting



from the wrong asymptotic behavior of the XC potentials make the improved correctly asymptotic XC functional compulsory.

Second, one of the deficiencies in TDDFT is related to the applied local XC functional that is not suited to describe nonlocal features such as charge separation.<sup>29,35–39</sup> Depending on the relative energies of orbitals and the molecular topology, the lowest excited-state either results from a HOMO  $\rightarrow$  LUMO ( $L_a$ ) excitation or is due to a mixture of the HOMO-1  $\rightarrow$  LUMO and HOMO  $\rightarrow$  LUMO+1 ( $L_b$ ) configurations. (By using the TDDFT calculations with the B3LYP functional below, we found that all the first dipole-allowed excited states of our investigated system were  $L_a$  states.) The  $L_a$  state has a large contribution from ionic valence-bond components in the wave function, while the  $L_b$  state is (similar to the ground state) mainly of covalent character.<sup>32,40,41</sup> According to the recent studies of large  $\pi$ -conjugated systems by Grimme and Parac,<sup>32,41</sup> the  $L_b$  state can be reproduced better with the conventional XC functional than the B3LYP functional. For the  $L_a$  state, however, the pure XC functional could lead to severe underestimates and the corresponding results of the hybrid-type B3LYP functional could well agree with the experimental data. The errors from using the pure XC functional are closely related to the ionic character of the  $L_a$  state that mainly originates from the charge transition between neighbor atoms or groups.<sup>41</sup> The work to create the separated charges in the  $L_a$  state is part of the excitation energy. Since the LDA potential only depends on the local density, the local XC potential cannot yield a counteracting term to adequately screen the ionic charges,<sup>35–38</sup> contrary to the case of the nonlocal HF potential.<sup>35,36</sup> So the local character of conventional XC functionals results in underestimated excitation energies. The same failure has also been pointed out for the calculation of polarizabilities with conventional functionals, a case of charge separation to chain ends in the whole molecule.<sup>35–38</sup> But, for the lowest-lying excitation energies, the case is not completely the same as that of polarizabilities. The underestimates using pure functionals are well correlated with the ionicity measure in the requirement of the summation restricted to interatomic distances larger than  $5a_0$  (2.6 Å). And the good correlation breaks down completely if the summation is restricted only to large distances (e.g.,  $> 10a_0$ ).<sup>41</sup> So the determinant regions of interaction energies of separated charges are between  $5a_0$  and  $10a_0$  for calculating lowest-lying excitation energies.<sup>41</sup> In addition, there are strongly system size dependent errors of polarizabilities,<sup>35–38</sup> whereas such dependent errors of lowest-lying excitation energies do not arise.<sup>21,28,33,41</sup> This fact also demonstrates that the charge interaction energies at large distances (e.g.,  $> 10a_0$ ) are not the determinants in the lowest-lying excitation energies. However, the nonlocal correction to the XC functional should also be necessary, although this intermediate region ( $5a_0$ – $10a_0$ ) is relatively “local” to the case of polarizabilities.

According to those mentioned above, an improved correctly asymptotic (at least correct in the spatial region related to the calculated energies) and nonlocal corrected XC functional must be applied. The B3LYP functional should be a good candidate for our investigated system to overcome these deficiencies. In the B3LYP functional, the exchange potential includes some percentage of the exact HF exchange, with the remain-

ing part being described by the Slater functional plus a weighted Becke gradient correction.<sup>42–44</sup> The third term of eq 1 just corresponds to the exact HF exchange.<sup>29,30</sup> On one hand, this term is essential for the correct  $1/r$  dependence of the interaction energies of ionic components in the  $L_a$  states,<sup>29</sup> while the incorrectly asymptotic functionals underestimate the interaction energies and result in the errors of excitation energies to lowest excited states.<sup>41</sup> An admixture with exact HF exchange can substantially improve the description of the  $L_a$  state.<sup>32</sup> On the other hand, since the HF exchange part is indeed nonlocal, the resulting XC potential yields a response to counteract the electric field resulting from charge separations. Such a response should undoubtedly arise in the exact XC potential, while it is not present in the LDA potential.<sup>35,36,38</sup> So the introduction of a nonlocal HF exchange part improves the ability of the XC functional to reproduce nonlocal features such as the intermediate-range charge separation. Hence, TDDFT with the B3LYP functional is expected to be a relatively reliable tool for evaluating the excitation energies of the lowest singlet excited states for the  $\pi$ -conjugated system we investigated.

There are two different theoretical approaches to evaluate band gaps of polymers. One is the polymer approach in which the periodic structures are assumed for infinite polymers. Another one is the oligomer extrapolation technique<sup>21</sup> that has acquired increasing popularity in this field. In this approach, a sequence of increasingly longer oligomers is calculated, and extrapolation to infinite chain length is followed. A distinct advantage of this approach is that it can provide the convergence behaviors of the structural and electronic properties of oligomers. In practice, both the polymer and the oligomer extrapolation approaches are generally considered to be complementary to each other in understanding properties of polymers. By considering the computational cost and the validity of TDDFT with the B3LYP functional simultaneously, we choose the oligomer extrapolation approach.

The calculations demonstrated in this paper were all obtained from the Gaussian 98 package.<sup>45</sup> First, ground-state geometric parameters (bond lengths and bond angles) of oligomers were fully optimized using the density functional theory (DFT) (B3LYP/6-31+G(d) as keyword), with the assumption of planar conformations under a constraint of inversion symmetry. Later on, B3LYP/6-31+G(d) calculations were performed at the optimized geometries of the ground states to calculate the excitation energies using TDDFT and the corresponding infrared spectra.

### 3. Results and Discussion

**3.1. Ground-State Energies.** So far as we judged from general knowledge, there should be two relatively stable, anticoplanar ground-state trans conformations of polyazopyrrole and polyazothiophene, respectively (as shown in Figure 2). By far, there is no report about the comparisons between them yet. It is necessary to first discern the most stable trans conformation that would be dominant in the corresponding infinite length polymer.

The HF ground-state energies of both  $n$ APY and  $n$ ATH decline as  $n$  increases (Table 1), which implies that the oligomers become more and more stable as the oligomer length increases. The energy difference ( $\Delta E_{\text{HF}n} = E_{\text{HF}nb} - E_{\text{HF}na}$ ) going up from the monomer

**Table 1. HF Ground-State Energies ( $E_{\text{HF}}/\text{au}$ ) of  $n\text{APY}a$ ,  $n\text{APY}b$ ,  $n\text{ATH}a$ , and  $n\text{ATH}b$  ( $n = 1-4$ ) and the Energy Difference ( $\Delta E_{\text{HF}}/\text{kJ}\cdot\text{mol}^{-1}$ ) between Conformation b and Conformation a**

	monomer		dimer		trimer		tetramer	
	a	b	a	b	a	b	a	b
$E_{\text{HF}}n\text{APY}/\text{au}$	-528.6412	-528.6351	-1056.0986	-1056.0853	-1583.5562	-1583.5357	-2111.0141	-2110.9862
$\Delta E_{\text{HF}}n\text{APY}^a/\text{kJ}\cdot\text{mol}^{-1}$	16.08		35.05		54.03		73.53	
$E_{\text{HF}}n\text{ATH}/\text{au}$	-1214.2963	-1214.2868	-2427.4045	-2427.3843	-3640.5141	-3640.4834	-4853.6238	-4853.5811
$\Delta E_{\text{HF}}n\text{ATH}^a/\text{kJ}\cdot\text{mol}^{-1}$	25.04		53.24		80.91		112.54	

$$^a \Delta E_{\text{HF}n} = E_{\text{HF}nb} - E_{\text{HF}na}.$$

**Table 2. Mulliken Charge Distribution, Bond Lengths ( $\gamma/\text{\AA}$ ), Bond Length Alternation (BLA), and Bond Alternation Parameters ( $\delta$ ) in the Middle Units of the  $n\text{APY}a$  ( $n = 1-4$ ) Chains**

	monomer	dimer	trimer	tetramer
Mulliken Charge Distribution				
$Q_{\text{C1}}$	0.530	0.237	0.116	0.088
$Q_{\text{C2}}$	-0.289	-0.406	-0.383	-0.372
$Q_{\text{C3}}$	-0.015	0.489	0.127	0.387
$Q_{\text{N4}}$	-0.452	-0.602	-0.516	-0.526
$Q_{\text{C5}}$	-0.560	-0.394	-0.201	-0.179
$Q_{\text{H6}}$	0.188	0.196	0.196	0.196
$Q_{\text{H7}}$	0.185	0.183	0.184	0.185
$Q_{\text{X8}}^a$	0.192	0.489	0.752	0.387
$Q_{\text{H9}}$	0.430	0.426	0.427	0.427
$Q_{\text{N10}}$	-0.207	-0.272	-0.215	-0.215
$Q_{\text{azo}}^b$	-0.414	-0.544	-0.430	-0.430
$Q_{\text{pyrroles}}^c$	0.414	0.618	0.652	0.639
Bond Lengths ( $\gamma/\text{\AA}$ ), Bond Length Alternation (BLA), and Bond Alternation Parameters ( $\delta$ )				
$\gamma_{\text{C1C2}}$	1.415	1.406	1.404	1.403
$\gamma_{\text{C2C3}}$	1.389	1.405	1.406	1.402
$\gamma_{\text{C3N4}}$	1.368	1.376	1.376	1.376
$\gamma_{\text{N4C5}}$	1.381	1.379	1.379	1.376
$\gamma_{\text{C5C1}}$	1.395	1.399	1.401	1.407
$\gamma_{\text{C1H6}}$	1.081	1.082	1.081	1.082
$\gamma_{\text{C2H7}}$	1.082	1.081	1.082	1.081
$\gamma_{\text{C3X8}}^a$	1.081	1.436	1.435	1.434
$\gamma_{\text{N4H9}}$	1.011	1.011	1.011	1.010
$\gamma_{\text{C5N10}}$	1.374	1.368	1.364	1.364
$\gamma_{\text{N10N11}}$	1.281	1.286	1.292	1.292
$\text{BLA}_{\text{C1C2C3}}$	0.026	0.001	-0.002	0.001
$\text{BLA}_{\text{C2C1C5}}$	0.020	0.007	0.003	-0.004
$\text{BLA}_{\text{N4C5N10}}$	0.007	0.011	0.015	0.012
$\delta_{\text{C1C2C3}}$	0.019	0.001	0.001	0.001
$\delta_{\text{C2C1C5}}$	0.014	0.005	0.002	-0.001
$\delta_{\text{N4C5N10}}$	0.005	0.008	0.011	0.009

<sup>a</sup> X = H in monomers, and X = C in other oligomers. <sup>b</sup> Mulliken charge sums of the azo group. <sup>c</sup> Mulliken charge sums of two pyrrole rings including X8 and X19.

to the tetramer demonstrates that conformation a would be a more energetically preferred conformation compared to conformation b and others. In view of the tendency of enhancing ratio of conformation a to conformation b with the augmentation of  $n$ , PAPY $a$  and PATH $a$  would be the dominant components in their corresponding ideal polymer bulks. So we will only analyze conformation a in detail in the following sections.

**3.2. Optimized Geometries.** The structural parameters of  $n\text{APY}a$  ( $n$  from 1 to 4) optimized by B3LYP/6-31+G(d) are given in Table 2. The sums of the Mulliken charges on the azo group and on the group of two pyrrole rings are negative and positive, respectively. The azo group shows an acceptor character. By inserting this group into the polypyrrole backbone, the alternate donor and acceptor moieties can be created. Such an acceptor/donor system is favorable for the reduction of the band gap.<sup>46</sup> That explicates the reason the inclusion of the azo group in the polypyrrole backbone can provoke a significant decrease in the band gap.

**Table 3. Mulliken Charge Distribution, Bond Length Alternation (BLA) and Bond Alternation Parameters ( $\delta$ ) in the Middle Units of the  $n\text{ATH}a$  ( $n = 1-4$ ) Chains**

	monomer	dimer	trimer	tetramer
$Q_{\text{azo}}^a$	0.026	-0.312	-0.134	-0.326
$Q_{\text{thiophenes}}^b$	-0.026	0.254	0.107	0.246
$\text{BLA}_{\text{C1C2C3}}$	0.044	0.016	0.011	0.010
$\text{BLA}_{\text{C2C1C5}}$	0.036	0.020	0.014	0.012
$\delta_{\text{C1C2C3}}$	0.032	0.011	0.008	0.007
$\delta_{\text{C2C1C5}}$	0.026	0.014	0.010	0.009

<sup>a</sup> Mulliken charge sums of the azo group. <sup>b</sup> Mulliken charge sums of two thiophene rings including X8 and X17.

In addition, by analyzing bond lengths  $\gamma$ , the reason for such a narrow band gap can also be explicated. It is known that the electronic delocalization structure is a representation of lowering the opening of a band gap in the Peierls distortion.<sup>8</sup> We use a bond alternation parameter  $\delta$  defined as  $(\gamma_{\text{C-C}} - \gamma_{\text{C=C}})/[(\gamma_{\text{C-C}} + \gamma_{\text{C=C}})/2]$ <sup>47,48</sup> to denote the degree of the electronic delocalization (as shown in Table 2). To facilitate the comparison with the bond length alternation (BLA), defined as the difference between double and single bond lengths<sup>49-51</sup> and usually used to represent the delocalization structure in many papers, these values are also listed in Table 2. It was reported that the  $\delta$  value of trans polyacetylene was about 0.06.<sup>48</sup> So the value  $\pm 0.02$  of  $\delta$  is a critical conjugation index to evaluate the strong electronic delocalization structure (Scheme 1 in ref 47). In Table 2 the  $\delta$  values of azopyrrole oligomers are all between -0.02 and 0.02 and BLA values are far below the 0.06 of polyacetylene. These results reveal that there is a strong electronic delocalization structure in these oligomers. So it is also not surprising that polyazopyrrole shows a narrow band gap.

In the same way, we can also reach the same conclusions for polyazothiophene from Table 3.

**3.3. Band Gaps.** Since the incorporated HF exchange-correlation potential decays correctly and simultaneously shows indeed nonlocal character, the asymptotic behavior and nonlocal property of the XC functional are expected to be better than those of uncorrected functionals, and TDDFT with the B3LYP functional is accordingly expected to properly reproduce the lowest singlet excited states of the investigated  $\pi$ -conjugated system. The TDDFT vertical excitation energies with the B3LYP functional of  $n\text{APY}$  and  $n\text{ATH}$  ( $n = 1-4$ ) are presented in Table 4. By plotting the results of the TDDFT vertical excitation energies of oligomers against the reciprocal of the number of repeat units  $n$  (Figure 3), we estimated the corresponding band gaps. Compared with the available experimental excitation energy for polyazopyrrole (about 1.0 eV<sup>11</sup>), the anticipated value of PAPY $a$  (1.12 eV) shows a good agreement. And the band gap of new PATH $a$  (0.98 eV) follows the anticipation of possessing a lower value than that of polyazopyrrole. It also shows a significant decrease in comparison with that of polythiophene (2.20 eV<sup>5</sup>). The above

**Table 4. HOMO–LUMO Gaps ( $\Delta_{\text{H-L}}$ /eV), the Negative of the HOMO Energies ( $-\epsilon_{\text{HOMO}}$ /eV), TDDFT Excitation Energies ( $E_{\text{TDDFT}}$ /eV), and Oscillator Strengths (in Parentheses) of *n*APYa and *n*ATHa (*n* = 1–4) with the B3LYP Functional**

		monomer	dimer	trimer	tetramer
<i>n</i> APYa	$\Delta_{\text{H-L}}$	3.1924	2.3020	1.9389	1.7583
	$-\epsilon_{\text{HOMO}}$	5.3783	4.9206	4.7523	4.6702
	$E_{\text{TDDFT}}$	3.2119	2.2579	1.8358	1.6022
		(0.8275)	(1.7200)	(2.6429)	(3.5104)
<i>n</i> ATHa	$\Delta_{\text{H-L}}$	3.2071	2.2082	1.8090	1.6022
	$-\epsilon_{\text{HOMO}}$	5.9965	5.5338	5.3620	5.2756
	$E_{\text{TDDFT}}$	3.1136	2.1520	1.7037	1.4819
		(0.6478)	(1.7765)	(2.8895)	(3.9437)

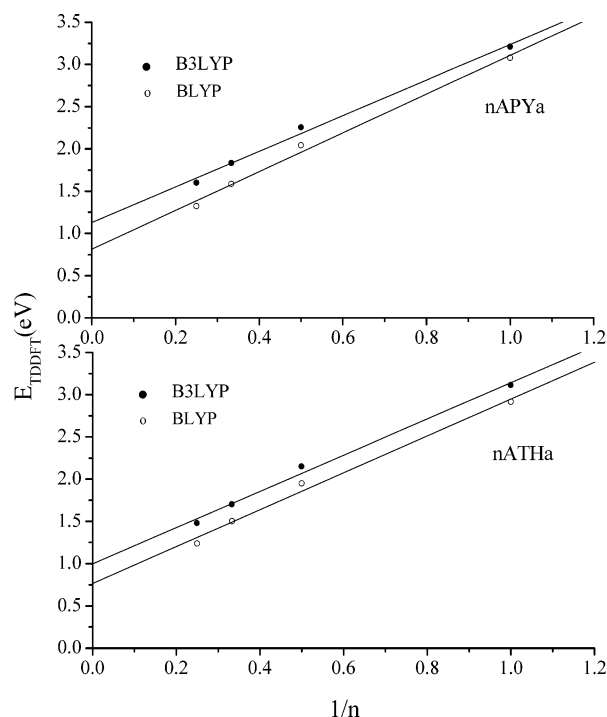


**Figure 3.** TDDFT vertical excitation energies of *n*APYa and *n*ATHa against the reciprocal of the number of repeat units *n*.

results may shed some light on developing and applying these azoheteroaromatic polymers in organic conductors, high nonlinear optical materials and IR-operating LEDs, and so forth.

To compare the performance of the hybrid-type B3LYP functional and that of the pure BLYP functional, the lowest-lying singlet excitation energies of *n*APYa and *n*ATHa (*n* = 1–4) were also calculated by using TDDFT with the BLYP functional (as shown in Figure 3). The extrapolated band gap of polyazopyrrole is 0.79 eV and is underestimated by 0.21 eV against the experimental one. So the introduction of the exact HF part can improve the performance of the functional and compensate the underestimates of interaction energies of separated charges. Such performances of the B3LYP and pure functionals are consistent with the studies of polycyclic aromatic hydrocarbons in ref 41.

It should also be noticed that excitation energies calculated by TDDFT with asymptotically incorrect functionals tend to collapse as they approach the negatives of the highest occupied orbital energies.<sup>26,33</sup> It is therefore necessary to check the validity of these excitation energies calculated by TDDFT with the B3LYP functional. In addition, it is also indispensable to compare the TDDFT excitation energies and the corre-

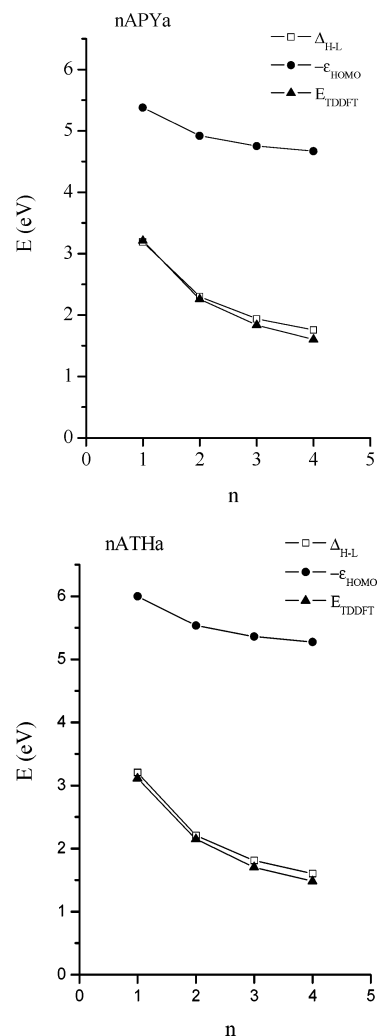


**Figure 4.** HOMO–LUMO gaps ( $\Delta_{\text{H-L}}$ ), the negative of the HOMO energies ( $-\epsilon_{\text{HOMO}}$ ), and TDDFT excitation energies ( $E_{\text{TDDFT}}$ ) of *n*APYa and *n*ATHa (*n* = 1–4) against the number of repeat units *n*.

sponding HOMO–LUMO gaps.<sup>30</sup> For all molecules under consideration, we have listed in Table 4 the negatives of the HOMO energies, the HOMO–LUMO gaps, and the TDDFT excitation energies. It can be seen from Figure 4 that in all cases the TDDFT excitation energies are far below the corresponding negatives of the HOMO energies. Furthermore, as the oligomer chain length increases, the TDDFT excited states lie lower than the negatives of the highest occupied energies. And the TDDFT excitation energies also do not show a tendency to converge to the same value with the corresponding HOMO–LUMO gaps. Hence, the incorrect asymptotic decay behavior of the approximate XC functional should have little influence and the calculated TDDFT excitation energies are numerically reliable.<sup>26,33</sup>

In addition, the agreement between the experimental and theoretical PAPY band gaps is well consistent with the former investigations by Salzner et al.<sup>28,52</sup> They have also used TDDFT with hybrid HF/DFT functionals to accurately predict (within 0.1 eV) the band gaps of many conducting polymers by oligomer extrapolating. So we hope the agreement between the experimental and theoretical band gaps of polyazopyrrole using TDDFT with the hybrid HF/DFT functional will restimulate the attention on this approach and similar results can also occur in more  $\pi$ -conjugated systems.

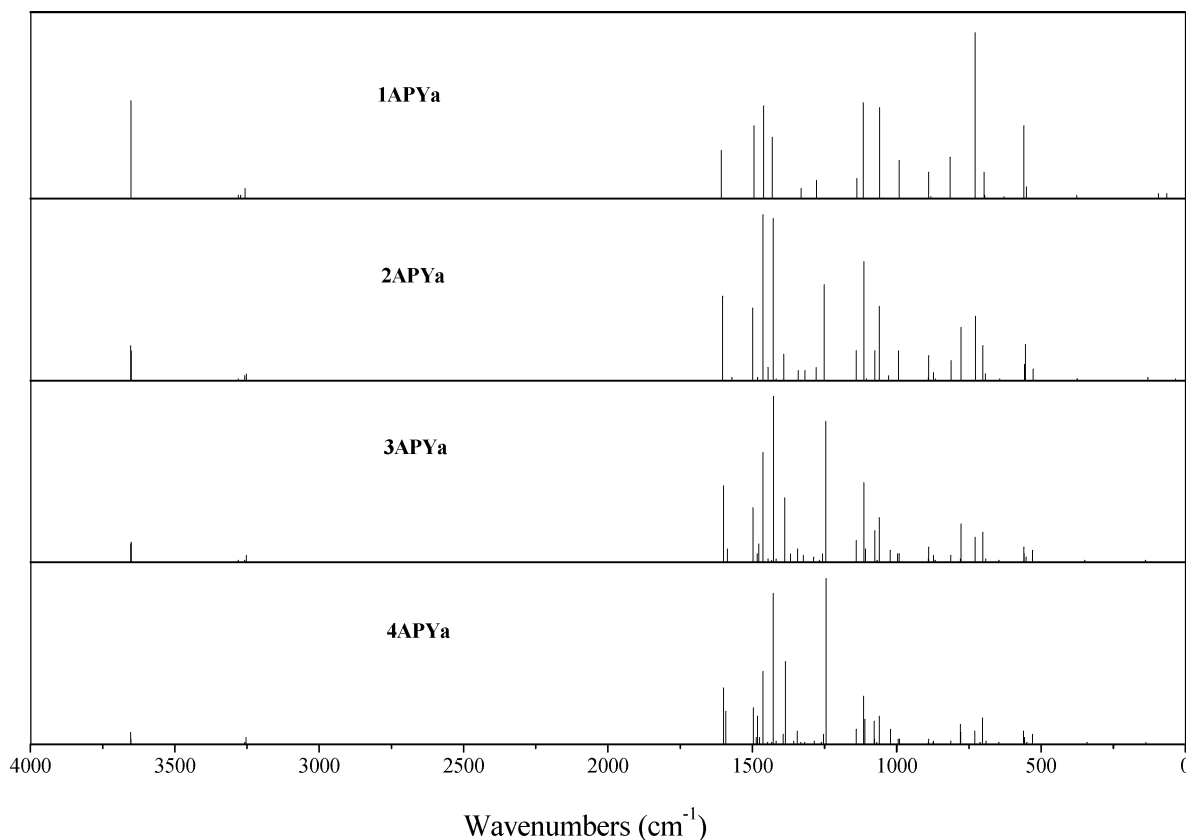


**Figure 5.** Calculated IR spectra of  $n$ APYn ( $n = 1-4$ ).

**3.4. ECLs.** Effective conjugation length (ECL) is a very useful concept, which can be represented as the number of repeat units at which saturation of a property occurs.<sup>53</sup> We estimated the ECLs based on the convergence of the calculated excited energy of the first dipole-allowed excited state with the increasing chain length. By extrapolating the resultant curve with the B3LYP functional to infinite chain length (Figure 3), the ECLs can be predicted. With the extension in the number of repeat units  $n$ , excitation energies of  $n$ APYn and  $n$ ATHa are estimated to be nearly constant within a threshold of 0.01 eV after 15 and 16 monomer units, respectively.

**3.5. Infrared Spectra.  $n$ APY.** We simulated the IR spectra of azopyrrole oligomers as shown in Figure 5. The bands of 1APYn are assigned as follows: C–N azo in-plane bending at 550  $\text{cm}^{-1}$ , C=C–N ring out-of-plane deformation at 560  $\text{cm}^{-1}$ , C=C–N ring in-plane deformation at 700  $\text{cm}^{-1}$ , C–H and N–H out-of-plane bending at 725 and 815  $\text{cm}^{-1}$ , C=C–C and C=C–N ring in-plane deformation at 890  $\text{cm}^{-1}$ , C–C, C=C, and C–N ring stretch at 990, 1055, 1115, 1140, 1275, 1330, 1430, 1460, 1495, and 1610  $\text{cm}^{-1}$ , C–H stretch at 3260  $\text{cm}^{-1}$ , N–H stretch at 3650  $\text{cm}^{-1}$ , respectively. The frequency positions of azopyrrole monomer are all well consistent with the previous experimental report except for the N–H stretch at 3650  $\text{cm}^{-1}$ , and the relative intensities seem to be analogous with those of the experimental spectrum (Figure 6). These results are also in good agreement with the judgment from the ground-state energies, indicating that  $n$ APYn would be a more energetically preferred conformation than others.

**$n$ ATH.** There is no report about the synthesis of azothiophene and its polymer yet. The good agreement with the experimental spectrum of azopyrrole indicates

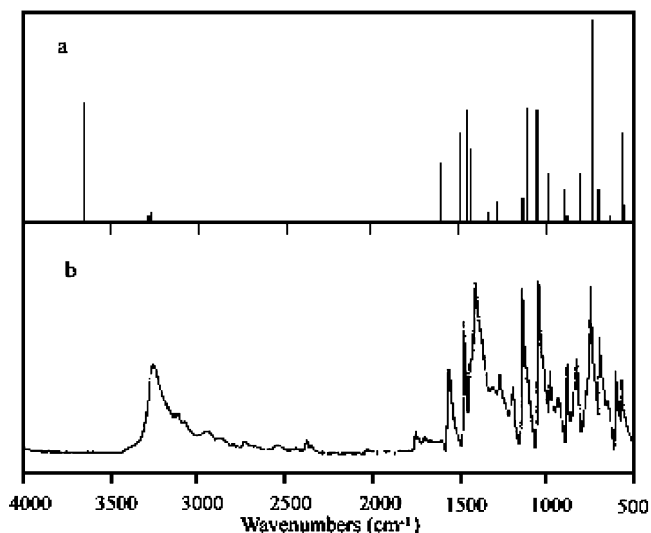


**Figure 6.** (a) Calculated and (b) experimental IR spectra of 1APYn. (The experimental IR spectrum is reprinted with permission from ref 11. Copyright 1996 Elsevier Science.)

that DFT with the B3LYP functional is a relatively reliable method for this system. So the IR spectra of the monomer and oligomers would be useful for the future syntheses and characterizations. The calculated IR spectra of  $n$ ATHa ( $n = 1-4$ ) are shown in Figure 7. The bands of 1ATHa are assigned as follows: C=C–C and C=C–S in-plane deformation at 553 and 1218  $\text{cm}^{-1}$ , C–S stretch at 484 and 704  $\text{cm}^{-1}$ , C–H out-of-plane bending at 713 and 850  $\text{cm}^{-1}$ , C–H in-plane bending at 1064  $\text{cm}^{-1}$ , C–C, C=C, C–S, and C–N stretch at 746, 861, 1289, 1410, 1474, and 1585  $\text{cm}^{-1}$ , C–H stretch at 3225  $\text{cm}^{-1}$ .



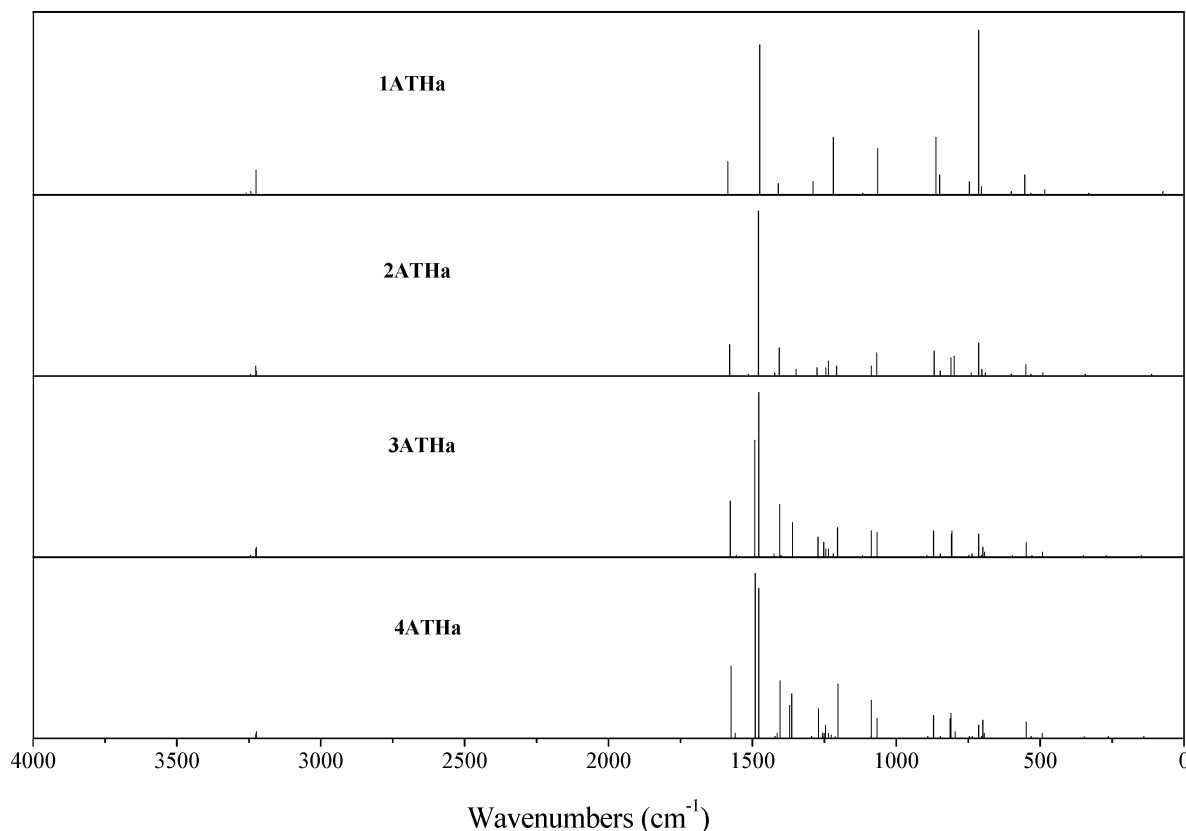


**Figure 7.** Calculated IR spectra of  $n$ ATHa ( $n = 1-4$ ).

#### 4. Conclusions

In this paper, we successfully used the hybrid DFT method B3LYP to investigate two narrow band gap polymers, polyazopyrrole and polyazothiophene. By comparing the HF ground-state energies, we discerned the most stable trans conformation that would be dominant in the corresponding infinite length polymer for the first time. We employed TDDFT with the B3LYP functional to study the chain length dependence of vertical excitation energies of azopyrrole and azothiophene oligomers from monomers to tetramers, and for the first time we theoretically predicted the band gaps of the corresponding infinite polyazopyrrole and polyazothiophene by extrapolation. The inclusion of the azo group in the polypyrrole and polythiophene backbone provoked significant decreases in band gaps from 2.85 to 1.12 eV and from 2.20 to 0.98 eV, respectively, characterizing them as potential narrow band gap materials. This kind of azoheteroaromatic polymers would be a promising candidate for molecular devices, high nonlinear optical materials, organic conductors and IR-operating LEDs, and so forth. In addition, we successfully simulated IR spectra of oligomers using the density functional theory (DFT) and estimated the effective conjugation lengths (ECLs) of the corresponding polymers. These results are in good agreement with experimental data where available.

**Acknowledgment.** We are grateful for the fruitful discussion with Prof. Martin Head-Gordon (Lawrence Berkeley National Laboratory) and Dr. Ma Jing (Nanjing University). The numerical calculations were carried out on the high-performance computers, SGI Origin 3800 and Dawning 3000A, of Nanjing University. This work was supported by the China NSFC (No.20174016).

#### References and Notes

- (1) Shirakawa, H.; Louis, E. J.; MacDiarmid, A. G.; Chiang, C. K.; Heeger, A. J. *Chem. Commun.* **1977**, 578.
- (2) Chiang, C. K.; Fincher, C. R., Jr.; Park, Y. W.; Heeger, A. J.; Shirakawa, H.; Louis, E. J. *Phys. Rev. Lett.* **1977**, *39*, 1098.
- (3) (a) Burroughes, J. H.; Bradey, D. D. C.; Brown, A. R.; Marks, R. N.; Mackay, K.; Friend, R. H.; Burn, P. L.; Holmes, A. B. *Nature* **1990**, *347*, 539. (b) Chen, W.; Wan, X. B.; Xu, N.; Xue, G. *Macromolecules* **2003**, *36*, 276. (c) Yan, F.; Xue, G.; Wan, F. *J. Mater. Chem.* **2002**, *12*, 2606. (d) Yan, F.; Xue, G. *J. Mater. Chem.* **1999**, *9*, 3035.
- (4) Kertesz, M. In *Handbook of Organic Conductive Molecules and Polymers*; Nalwa, H. S., Ed.; John Wiley & Sons Ltd.: New York, 1997; Vol. 4, pp 147-172.
- (5) Roncali, J. *Chem. Rev. (Washington, D. C.)* **1997**, *97*, 173-205.
- (6) Baigent, D. R.; Hamer, P. J.; Friend, R. H.; Moratti, S. C.; Holmes, A. B. *Synth. Met.* **1995**, *71*, 2175.
- (7) Wennerstroem, O. *Macromolecules* **1985**, *18*, 1977.
- (8) Peierls, R. E. *Quantum Theory of Solids*; Clarendon: Oxford, 1956.
- (9) Groenendaal, L.; Jonas, F.; Freitag, D.; Pielartzik, H.; Reynolds, J. R. *Adv. Mater.* **2000**, *12*, 481.
- (10) Yokomichi, Y.; Seki, K.; Tada, S.; Yamabe, T. *Synth. Met.* **1995**, *69*, 577.
- (11) Zotti, G.; Zecchin, S.; Schiavon, G.; Berlin, A.; Pagani, G.; Canavesi, A.; Casalbore-Miceli, G. *Synth. Met.* **1996**, *78*, 51.
- (12) Zotti, G.; Martina, S.; Wegner, G.; Schlüter, A.-D. *Adv. Mater.* **1992**, *4*, 798.
- (13) Nero, J. D.; Laks, B. *Synth. Met.* **1999**, *101*, 440.
- (14) Pieroni, O.; Fissi, A.; Angelini, N.; Lenci, F. *Acc. Chem. Res.* **2001**, *34*, 9.
- (15) Liu, Z. F.; Hashimoto, K.; Fujishima, A. *Nature* **1990**, *347*, 658.
- (16) De Oliveira, M. A.; Duarte, H.; Pernaut, J.; De Almeida, W. B. *J. Phys. Chem. A* **2000**, *104*, 8256.
- (17) Salzner, U.; Lagowski, J. B.; Pickup, P. G.; Poirier, R. A. *Synth. Met.* **1998**, *96*, 177.
- (18) Foresman, J. B.; Head-Gordon, M.; Pople, J. A.; Frisch, M. J. *J. Phys. Chem.* **1992**, *96*, 135.
- (19) Dunning, T. H.; McKoy, V. *J. Chem. Phys.* **1967**, *47*, 1735.
- (20) Jorgensen, P. *Annu. Rev. Phys. Chem.* **1975**, *26*, 359.
- (21) Ma, J.; Li, S.; Jiang, Y. *Macromolecules* **2002**, *35*, 1109.

- (22) Koch, W.; Holthausen, M. C. *A Chemist's Guide to Density Functional Theory*, 2nd ed.; Wiley-VCH: Germany, 2001.
- (23) Casida, M. E. *Recent Advances in Density Functional Methods, Part I*; World Scientific: Singapore, 1995.
- (24) Sundholm, D. *Chem. Phys. Lett.* **1999**, *302*, 480.
- (25) Dreuw, A.; Dunietz, B. D.; Head-Gordon, M. *J. Am. Chem. Soc.* **2000**, *122*, 1717.
- (26) Casida, M. E.; Jamorski, C.; Casida, K. C.; Salahub, D. R. *J. Chem. Phys.* **1998**, *108*, 4439.
- (27) Cavillot, V.; Champagne, B. *Chem. Phys. Lett.* **2002**, *354*, 449.
- (28) Salzner, U.; Pickup, P. G.; Poirier, R. A.; Lagowski, J. B. *J. Phys. Chem. A* **1998**, *102*, 2572.
- (29) Dreuw, A.; Weisman, J. L.; Head-Gordon, M. *J. Chem. Phys.* **2003**, *119*, 2943.
- (30) Hirata, S.; Head-Gordon, M.; Bartlett, R. J. *J. Chem. Phys.* **1999**, *111*, 10774.
- (31) van Leeuwen, R.; Baerends, E. J. *Phys. Rev. A* **1994**, *49*, 2421.
- (32) Grimme, S.; Parac, M. *ChemPhysChem* **2003**, *3*, 292.
- (33) Hsu, C. P.; Hirata, S.; Head-Gordon, M. *J. Phys. Chem. A* **2001**, *105*, 451.
- (34) Tozer, D. J.; Handy, N. C. *J. Chem. Phys.* **1998**, *109*, 10180.
- (35) Champagne, B.; Perpete, E. A.; Jacquemin, D.; van Gisbergen, S. J. A.; Baerends, E. J.; Soubra-Ghaoui, C.; Robins, K. A.; Kirtman, B. *J. Phys. Chem. A* **2000**, *104*, 4755.
- (36) van Gisbergen, S. J. A.; Schipper, P. R. T.; Gritsenko, O. V.; Baerends, E. J.; Snijders, J. G.; Champagne, B.; Kirtman, B. *Phys. Rev. Lett.* **1999**, *83*, 694.
- (37) Champagne, B.; Perpete, E. A.; van Gisbergen, S. J. A.; Baerends, E. J.; Snijders, J. G.; Soubra-Ghaoui, C.; Robins, K. A.; Kirtman, B. *J. Chem. Phys.* **1998**, *109*, 10489.
- (38) van Faassen, M.; de Boeij, P. L.; van Leeuwen, R.; Berger, J. A.; Snijders, J. G. *Phys. Rev. Lett.* **2002**, *88*, 186401.
- (39) Paddon-Row, M. N.; Shephard, M. J. *J. Phys. Chem. A* **2002**, *106*, 2935.
- (40) Platt, J. R. *J. Chem. Phys.* **1949**, *17*, 484.
- (41) Parac, M.; Grimme, S. *Chem. Phys.* **2003**, *292*, 11.
- (42) Becke, A. D. *Phys. Rev. A* **1988**, *38*, 3098.
- (43) Lee, C.; Yang, W.; Parr, R. G. *Phys. Rev. B* **1988**, *37*, 785.
- (44) Becke, A. D. *J. Chem. Phys.* **1993**, *98*, 5648.
- (45) GAUSSIAN 98; Gaussian, Inc.: Pittsburgh, PA, 1998.
- (46) Havinga, E. E.; Hoeve, W. T.; Wynberg, H. *Polym. Bull.* **1992**, *29*, 119.
- (47) Zhang, G.; Ma, J.; Jiang, Y. *Macromolecules* **2003**, *36*, 2130.
- (48) Curran, S.; Stark-Hauser, A.; Roth, S. In *Handbook of Organic Conductive Molecules and Polymers*; Nalwa, H. S., Ed.; John Wiley & Sons Ltd.: New York, 1997; Vol. 2, p 14.
- (49) Bredas, J. L. *J. Chem. Phys.* **1985**, *82*, 3808.
- (50) Jacquemin, D.; Perpete, E. A.; Champagne, B. *Phys. Chem. Chem. Phys.* **2002**, *4*, 432.
- (51) Bartkowiak, W.; Zalesny, R.; Leszczynski, J. *Chem. Phys.* **2003**, *287*, 103.
- (52) Salzner, U.; Lagowski, J. B.; Pickup, P. G.; Poirier, R. A. *J. Comput. Chem.* **1997**, *18*, 1943.
- (53) Martin, R.; Diederich, F. *Angew. Chem., Int. Ed.* **1999**, *38*, 1350.

MA034564+